Chinese Journal of Integrative Medicine
Available online at link.springer.com/journal/11655
Journal homepage: www.cjim.cn/zxyjhen/zxyjhen/ch/index.aspx
E-mail: cjim_en@cjim.cn

Original Article

Protective Effect of Ganshuang Granules (肝爽颗粒) on Liver Cirrhosis by Suppressing Regulatory T Cells in Mouse Model*

LIU Yan-min[1], SHI Hong-bo[1,2], LIU Yi-rong[3], SHI Hong-lin[1,2], REN Feng[1,2], CHEN Yu[4], CHEN De-xi[1,2], LOU Jin-li[5], and DUAN Zhong-ping[4]

ABSTRACT **Objective**: To investigate the potential antifibrotic mechanisms of Chinese medicine Ganshuang Granules (肝爽颗粒, GSG) and to provide clinical therapeutic evidence of its effects. **Methods**: A cirrhotic mouse model was established by intraperitoneally injecting a mixture of CCl_4 (40%) and oil (60%) at 0.2 mL per 100 g of body weight twice a week for 12 weeks. After 12-week modeling, GSG was intragastric administrated to the mice for 2 weeks, and the mice were divided into low-, medium- and high-dose groups at doses of 1, 2 and 4 g/(kg·day), respectively. Liver morphology changes were observed using Masson's trichrome staining and B-ultrasound. The levels of alanine aminotransferase (ALT), aspartate aminotransferase (AST) and hyaluronic acid (HA) in serum were detected using an automatic biochemistry analyzer. The expressions of desmin, smooth muscle actin (SMA) and Foxp3 in liver were detected by immunofluorescence. The regulatory T cell (Treg) frequency was determined through flow cytometry analysis. Collagen-Ⅰ, SMA, IL-6, tumor necrosis factor α (TNF-α), interleukin (IL)-1β and transforming growth factor β1 (TGF-β1) expression levels were measured using quantitative polymerase chain reaction (qPCR). **Results**: Masson's staining result showed fewer pseudolobule structures and fibrous connective tissue in the GSG-treatment groups than in the spontaneous recovery group. Ultrasonography showed that GSG treatment reduced the number of punctate hyperechoic lesions in mice cirrhotic livers. The serum ALT, AST, HA levels were significantly ameliorated by GSG treatment (ALT: F=8.104, P=0.000; AST: F=7.078, P=0.002; and HA: F=7.621, P=0.001). The expression levels of collagen-Ⅰ and SMA in the cirrhotic livers were also attenuated by GSG treatment (collagen-Ⅰ: F=3.938, P=0.011; SMA: F=4.115, P=0.009). Tregs, which were elevated in the fibrotic livers, were suppressed by GSG treatment (F=8.268, P=0.001). The expressions of IL-6, TNF-α and IL-1β increased, and TGF-β levels decreased in the cirrhotic livers after GSG treatment (IL-6: F=5.457, P=0.004; TNF-α: F=6.023, P=0.002; IL-1β: F=6.658, P=0.001; and TGF-β1: F=11.239, P=0.000). **Conclusions**: GSG promoted the resolution/regression of cirrhosis and restored liver functions in part by suppressing Treg cell differentiation, which may be mediated by hepatic stellate cells.

KEYWORDS Ganshuang Granules, liver cirrhosis, regulatory T cell, hepatic stellate cell, Chinese medicine

Cirrhosis, which is a common consequence of chronic liver diseases regardless of the cause, decreases parenchymal function and creates an environment that is compatible with tumors. Cirrhosis and its disease-related complications are the main causes of mortality among Chinese adults and are the first leading causes of death for middle-aged males. Hospitalization costs for disease-related complications are estimated at $18,000 per episode of care, and 10% of admitted patients die.[1] Moreover, there are few effective and specific treatments or medications for cirrhosis.[2] Some Chinese medicine (CM) herbs or prescriptions, which have long been used in clinical practice based on CM theory, may

*Supported by the China National Key Project of Twelfth Five-Year Plan (Nos. 2012ZX10002004-006, 2012ZX10004904-003-001, and 2013ZX10002002-006-001), National Natural Science Foundation of China (No. 81300349), Beijing Natural Science Foundation (No. 7144216), Beijing Nova Program (No. Z131107000413016), and Project of Science and Technology Activities Preferred Overseas Personnel of Beijing (No. 2014)
1. Department of Liver Diseases Immunology, Beijing Youan Hospital, Capital Medical University, Beijing (100069), China; 2. Beijing Institute of Hepatology, Beijing Youan Hospital, Capital Medical University, Beijing (100069), China; 3. Department of Toxic Hepatic Disease, Beijing Youan Hospital, Capital Medical University, Beijing (100069), China; 4. Artifical Liver Center, Beijing Youan Hospital, Capital Medical University, Beijing (100069), China; 5. Clinical Laboratory Center, Beijing Youan Hospital, Capital Medical University, Beijing (100069), China
Correspondence to: Dr. DUAN Zhong-ping, Tel: 86-10-63291007, E-mail: duan2517@163.com
DOI: https://doi.org/10.1007/s11655-015-2430-9

Chin J Integr Med 2019 Jan;25(1):51-58

offer hope in treating cirrhosis.[3,4] Ganshuang Granules (肝爽颗粒, GSG) has been used to treat various chronic liver diseases. According to CM theory, GSG functions by protecting the Gan (Liver), strengthening the Pi (Spleen), clearing heat and stasis and resolving hard lumps.

A previous study has demonstrated that GSG played an antifibrotic role, partially by suppressing the activation of hepatic stellate cells (HSCs).[5,6] However, the mechanism through which GSG protects the cirrhotic liver is unknown. Recent reports have demonstrated that activated HSCs preferentially induce regulatory T cell (Treg) differentiation by producing retinoic acid.[7] We hypothesized that GSG may play an important antifibrotic role by influencing Treg differentiation and proliferation. Thus, the aims of this study were to investigate the potential antifibrotic mechanisms of GSG and to provide clinical therapeutic evidence of its effects. It is necessary to verify the effectiveness of this antifibrotic role and the underlying mechanisms for GSG before its large-scale clinical use.

METHODS

Animals

Male Balb/c mice (4–6 weeks of age; weight, 25–30 g; specific pathogen free) were provided by the Animal Center at the Academy of Military Medical Sciences, China [certification No. SCXK (Army) 2007-004]. All animals were placed in a pathogen-free environment and maintained in 12-h dark/light cycles at 22–24 ℃ and 30%–40% humidity. The study protocol was approved by the Ethics Committee at Beijing Youan Hospital, Capital Medical University, China.

GSG

GSG was developed by the Buchang Pharmacy Limited Company, Xi'an, China. GSG is composed of 13 herbs: *Salvia miltiorrhiza* Bge, *Radix Bupleuri*, *Radices paeoniae alba*, *Angelica sinensis*, *Poria cocos*, *Atractylodes macrocephala Koidz*, *Fructus Aurantii*, *Taraxacum mongolicum*, *Polygonum cuspidatum*, *Prunella vulgaris* Linn, *Codonopsis pilosula*, *Semen Persicae* and *Carapax Trionycis*. The chemical pattern was analyzed with high performance liquid chromatography (HPLC, Waters 2695, USA) with UV detection at 210 nm. The analysis was performed with a CAPCELL PAK C18 MG column (250 mm × 4.6 mm × 5 μm, Shiseido, Japan) at 40 ℃. The compounds were eluted (elution buffer A, water; elution buffer B, acetonitrile) at a flow rate of 1 mL/min using a gradient program. As illustrated in Figure 1, the main peaks in the HPLC fingerprint were identified as paeoniflorin (peak 1, 2.224 mg/g), polydatin (peak 2, 1.557 mg/g), ferulic acid (peak 3, 0.733 mg/g), naringin (peak 4, 6.128 mg/g), neohesperidin (peak 5, 2.783 mg/g), saikosaponin a (peak 6, 0.039 mg/g),

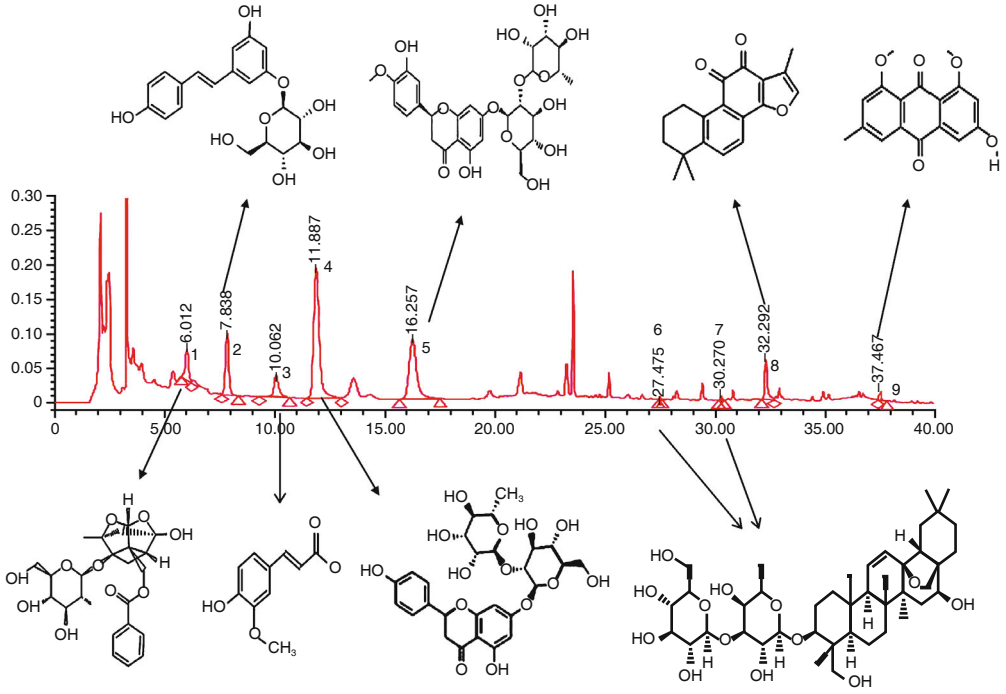

Figure 1. Chemical Profile of GSG Analyzed by HPLC

saikosaponin d (peak 7, 0.469 mg/g), tanshinone ⅡA (peak 8, 0.484 mg/g), and emodin (peak 9, 0.102 mg/g).

Experimental Design

Forty mice were randomly divided into a model group (n=28) and a normal control group (n=7) by a random number table. The model group was intraperitoneally injected with a mixture of CCl_4 (40%) and oil (60%) at a dose of 2 mL/kg body weight twice a week for 12 weeks. The normal control group was injected the same volume of oil at the same time and position as the model group. At week 12, the model mice were further randomly divided into 4 groups by a random number table (n=7 in each group) that were subjected to additional treatment for 2 weeks: the GSG low-, medium-, and high-dose groups, which were intragastric administrated with GSG at the dose of 1, 2, 4 g/(kg·day), respectively, once daily; and the spontaneous recovery (SR) group, which was fed a volume of distilled water equal to the volume of GSG.

Sample Collection and Detection

The mice were anesthetized with chloral hydrate and fixed in a supine position. Their abdominal cavities were opened, and approximately 1 mL of postcaval vein blood was collected. The left lobe of the liver was excised and fixed in 4% neutral buffered formalin for 24 h and embedded in paraffin; then, 4-μm thick sections were sliced with a microtome for Masson's and immunofluorescence staining. The other liver tissue was rinsed in saline solution for flow cytometry analysis. The serum levels of alanine aminotransferase (ALT), aspartate aminotransferase (AST) and hyaluronic acid (HA) were detected by the Clinic Center of Beijing Youan Hospital using an automatic biochemistry analyzer. Liver fibrosis and cirrhosis in animate mice were detected using ultrasound by basic clinical researchers at Capital Medical University.

Masson Trichrome Staining

The samples were deparaffinized and rehydrated with 100%, 95% and 70% alcohol. The samples were then washed in distilled water and rinsed in running tap water for 5–10 min before staining in Biebrich scarlet-acid fuchsin solution for 10–15 min, washed in distilled water and differentiated in phosphomolybdic-phosphotungstic acid solution for 10–15 min or until the collagen was not red. The sections were transferred directly (without rinsing) to an aniline blue solution and stained for 5–10 min before being rinsed briefly in distilled water and differentiated in 1% acetic acid solution for 2–5 min. Then, the samples were washed in distilled water and dehydrated quickly with 95% ethyl alcohol, absolute ethyl alcohol and clear in xylene. The samples were then mounted with resinous mounting medium.

Immunofluorescence

The sections were blocked with a blocking buffer (5% goat serum and 0.2% bovine serum albumin) at room temperature for 30 min and then washed 3 times with phosphate buffered saline (PBS). The primary antibody anti-smooth muscle actin [anti-smooth muscle actin (SMA) and anti-desmin or anti-Foxp3, Abbiotec, 1:400] was applied at room temperature for 1 h. Then, the samples were washed, and the secondary antibody [goat anti-mouse and goat anti-rabbit F(ab')2 fragment of IgG (H+L) antibody, Invitrogen, 1:400] was applied at room temperature for 30 min. The sections were counterstained with 6-diamidino-2-phenylindole (DAPI). All images were obtained using an inverted fluorescence microscope (Nikon Eclipse E800, Japan).

Flow Cytometry Analysis

After partial digestion of the whole liver lobes with 10 mg/mL Ⅳ collagenase (Worthington, USA) and 50 U/mL DNase Ⅰ (Sigma, USA) in DMEM/F-12 medium for 40 min at 37 ℃ with gentle shaking, the cells were centrifuged at 30×g for 10 min. The supernatant was centrifuged at 1,100×g for 10 min, and the cells were gently added into lymphocyte separation liquid. The middle layer was isolated and washed three times with cold PBS. The cells were stained with anti-mouse CD4 FITC and anti-mouse CD25 PECy5 (eBioscience, USA) at room temperature for 20 min. A perm buffer was added to the cells at room temperature for 45 min. The cells were stained with anti-mouse Foxp3-PE (eBioscience, USA) at room temperature for 30 min. The cells were evaluated using flow cytometry (BD FACSCalibur, USA).

Quantitative Polymerase Chain Reaction

Total RNA was extracted using the TRIzol kit (Invitrogen, USA), according to the manufacturer's instructions. The first strand cDNA was synthesized from 5 μg of RNA (Superscript Ⅲ cDNA Synthesis Kit, Invitrogen), and the mRNA levels of collagen-Ⅰ, SMA, interleukin (IL)-6, tumor necrosis factor α (TNF-α), IL-1β, transforming growth factor β1 (TGF-β1) and glyceraldehyde 3-phosphate dehydrogenase (GADPH) were determined by quantitative polymerase chain reaction (qPCR) using the SYBR Green PCR

Chin J Integr Med 2019 Jan;25(1):51-58

Kit (Invitrogen) in a real-time PCR system (ABI PRISM7300, USA). The relative quantification cycle threshold (CT) value for each primer was normalized to the internal primer. The △CT was calculated as the difference between the CT values of the target gene and the internal gene. The $2^{-\triangle CT}$ value was acquired and compared among the groups.

Statistical Analyses

One-way analysis of variance (ANOVA), followed by a post hoc LSD test, was used to compare the differences between multiple groups, and *P* values less than 0.05 were considered significant. All data were analyzed with SPSS software, version 11.5.

RESULTS

Protective Effect of GSG on Liver Fibrosis and Cirrhosis in Mice

As shown in Figure 2, compared with the SR group, the mice treated with GSG had fewer punctate hyperechoic lesions on the B-ultrasound picture, particularly in the high-dose group; Masson's staining showed the same trend. In addition, other markers of liver fibrosis provided further evidence. The difference in the HA levels among groups was significant (*F*=7.621, *P*=0.001), and the HA level in the SR group was higher than that in the high-, medium- and low-dose groups (*P*=0.017, 0.033, 0.489, respectively). These results showed that the level of fibrosis in the SR group was higher than that in the GSG-treatment groups.

Another protective role of GSG was verified. The difference between the ALT and AST levels among groups was significant (ALT: *F*=8.104, *P*=0.000; AST: *F*=7.078, *P*=0.002), and the levels of ALT and AST in the SR group were higher than that in the high-, medium- and low-dose groups (ALT: *P*=0.009, 0.008, 0.018, respectively; AST: *P*=0.001, 0.003, 0.001, respectively; Figure 3).

Suppressive Effect of GSG on Activation of HSCs and Tregs in Cirrhotic Mice

As shown in Figure 4, compared with the SR group, the expression of SMA was decreased, and there was less nuclear deformation and disordered structure in the liver tissues of the mice in the GSG treatment groups. Surprisingly, as double staining of Foxp3 and SMA was performed, it was found that the expression of

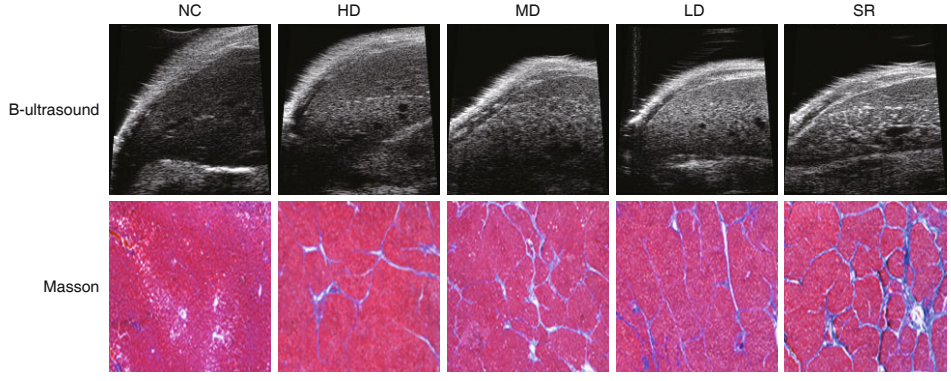

Figure 2. Liver Fibrosis and Cirrhosis in Mice Detected Using B-ultrasound and Masson's Staining (× 40)

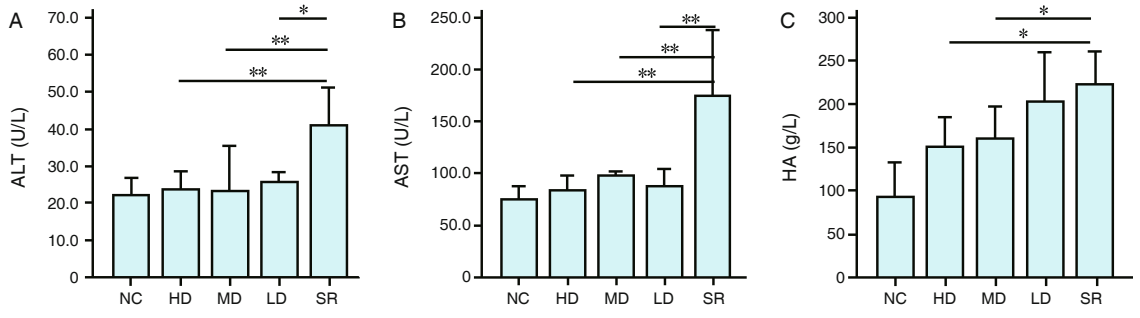

Figure 3. Comparison of ALT (A), AST (B) and HA (C) Levels in Serum of Cirrhotic Mice among Groups

Notes: NC: normal control; HD: GSG high-dose group; MD: GSG medium-dose group; LD: GSG low-dose group; SR: spontaneous recovery group; $^{*}P<0.05$, $^{**}P<0.01$; the same below

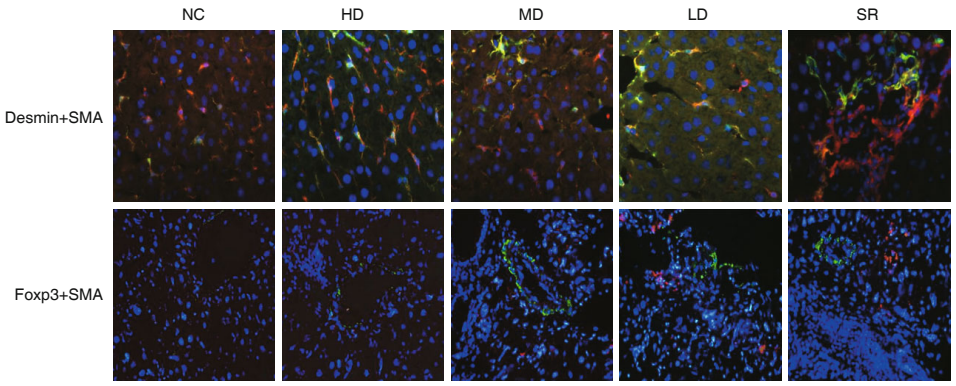

Figure 4. Expression Levels of Desmin and SMA and Foxp3 and SMA in Mice Liver Detected by Immunofluorescence

Notes: Magnification: ×100 for desmin and SMA and ×40 for Foxp3 and SMA

Foxp3 increased in conjunction with the increase in SMA expression, and vice versa. The difference in the mRNA expression of collagen-Ⅰ and SMA among groups was significant (collagen-Ⅰ: F=3.938, P=0.011; SMA: F=4.115, P=0.009), and the expression of collagen-Ⅰ and SMA in the SR group was higher than those in the high-, medium- and low-dose GSG groups (collagen-Ⅰ: P=0.004, 0.03, 0.102, respectively; SMA: P=0.007, 0.005, 0.008, respectively; Figure 5).

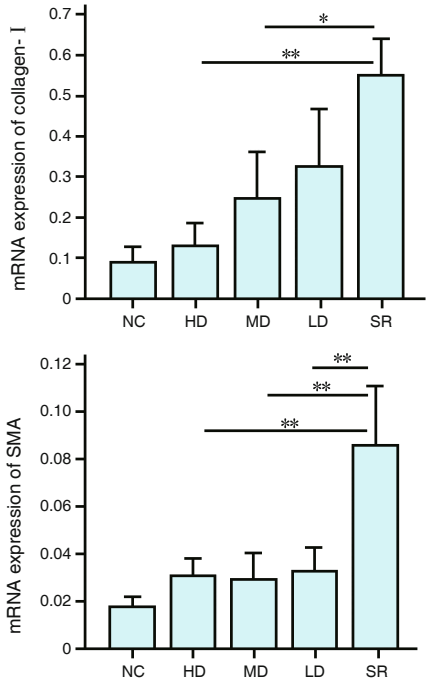

Figure 5. Comparison of mRNA Expression of Collagen-Ⅰ and SMA of Cirrhotic Mice among Groups Measured by qPCR

Suppressive Effect of GSG on Differentiation of Treg Cells in Cirrhotic Mouse Model

As shown in Figure 6, the difference of Treg cell frequency in mouse liver among groups was significant (F=8.268, P=0.001), and it was higher in the SR group than in the high-, medium- and low-dose GSG groups (P=0.002, 0.021, 0.278, respectively). As for the mRNA level, the difference of Foxp3 expression among the groups had significance (F=16.635, P=0.000), and the Foxp3 expression in the SR group was higher than that in the high-, medium- and low-dose GSG groups (P=0.000, 0.008, 0.328, respectively; Figure 7).

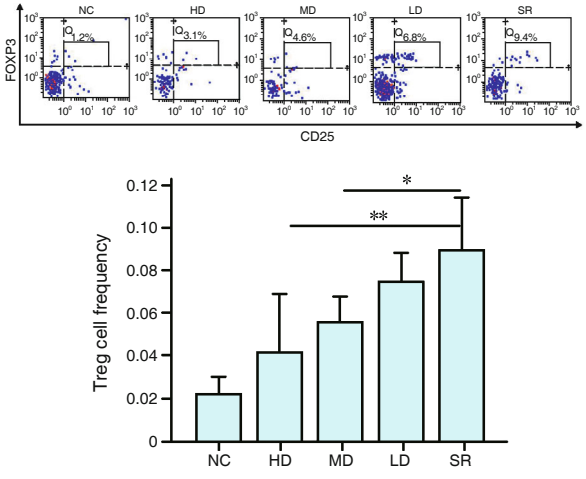

Figure 6. Suppressive Effect of GSG on Differentiation of Treg Cells in Cirrhotic Mice by Flowcytometry

Effect of GSG on Expression of Different Cytokines in Cirrhotic Mouse Model

In our study, the differences in the expression levels of IL-6, TNF-α, IL-1β and TGF-β1 among the groups were significant (IL-6: F=5.457, P=0.004; TNF-α: F=6.023, P=0.002; IL-1β: F=6.658, P=0.001; TGF-β1: F=11.239, P=0.000), and the

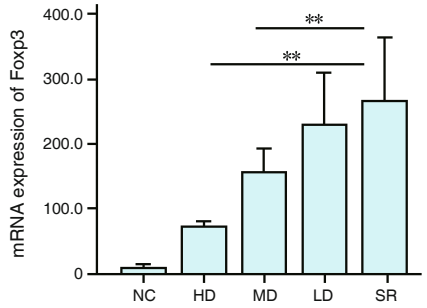

Figure 7. Comparison of mRNA Expression of Foxp3 among Groups Measured by qPCR

expression levels of IL-6, TNF-α, and IL-1β in the SR group were lower than those in the GSG high-medium-, and low-dose groups (IL-6: *P*=0.010, 0.031, 0.599, respectively; TNF-α: *P*=0.003, 0.020, 0.359, respectively; IL-1β: *P*=0.000, 0.060, 0.401, respectively), and the expression of TGF-β1 showed the opposite result (*P*=0.000, 0.003, 0.059, respectively; Figure 8).

DISCUSSION

Although pathological detection is the gold standard for diagnosis of liver fibrosis, the procedures only involve observing a section of the liver, whereas B-ultrasound can scan the entire liver. Therefore we combined B-ultrasound and pathological detection to analyze the level of liver fibrosis and cirrhosis. We observed many punctate hyperechoic lesions on the B-ultrasound picture, which was generated by CCl_4 exposure for 12 weeks. Moreover, substantial amounts of fibrous connective tissue and complete pseudolobules were present in the Masson's staining. Together, the evidence suggested that the cirrhotic model was successfully established.

Comprehensive studies have demonstrated that cirrhosis, to a certain extent, can be resolved or regressed if hepatic infection or injury is controlled.[8] Similar to these studies, we observed more fibrous connective tissue in the SR group than in the GSG-treatment groups, the levels of ALT and AST in the SR group were higher than those in the GSG-treatment groups, and the level of HA in the SR group was higher than those in the GSG-treatment groups, suggesting that the GSG treatment exerted a protective effect on liver fibrosis or cirrhosis, which can improve liver function and decrease the level of fibrosis.

HSC activation is considered as a major mechanism in the formation of fibrosis and cirrhosis.

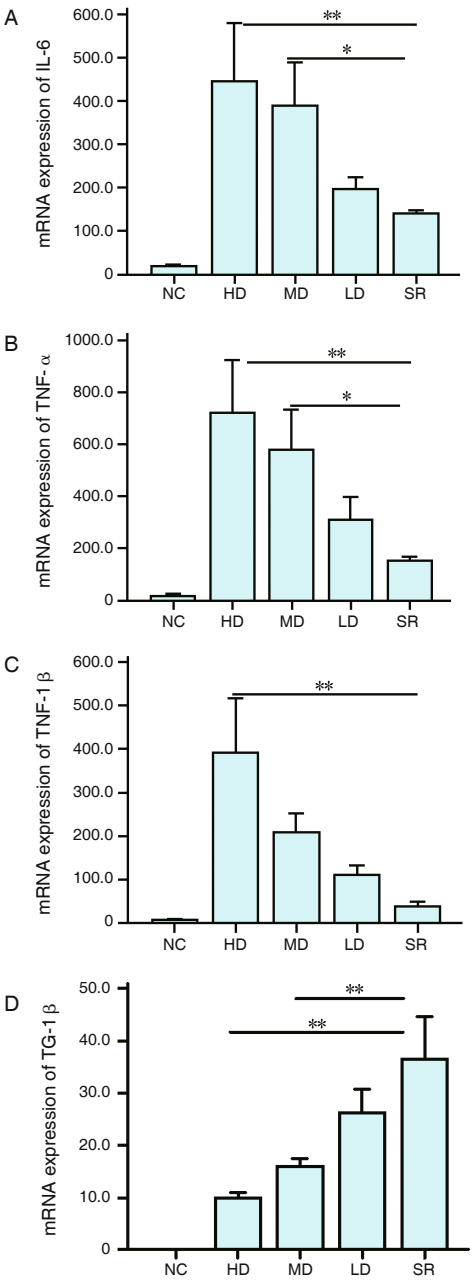

Figure 8. mRNA Expression Levels of IL-6 (A), TNF-α (B), IL-1β (C) and TGF-β1 (D) in Mice Liver Measured by qPCR

Note that HSCs, which are located in the space of Disse in the liver, play a pivotal role in the development of liver fibrosis and cirrhosis.[9,10] In normal adult liver, quiescent HSCs are characterized by desmin expression, vitamin A storage, and extensive dendrite-like processes. Upon injury, HSCs are activated, lose vitamin A lipids and transform into a myofibroblastic phenotype expressing SMA and excessive extracellular matrix proteins.[11-13] Consistent with other studies, we found that the expression of SMA and collagen-Ⅰ in mouse liver in the GSG-treatment groups were

lower than that in the SR group, which indicated that GSG can suppress HSC activation. GSG may play an important antifibrotic role by suppressing HSC activation. In addition, surprisingly, we found that Foxp3 expression increased in conjunction with increases in SMA expression, and vice versa, indicating that GSG promoted the resolution/regression of cirrhosis and restored liver functions, in part by suppressing Treg cell differentiation, which may be mediated by HSCs.

HSCs have been associated with the production of both retinoic acid and TGF-β1. HSCs are the primary storage cell for retinol (vitamin A), which is metabolized to retinoic acid during activation, and activated HSCs have also been shown to produce TGF-β1.[14,15] Note that naive $CD4^+$T cells can be primed to become $CD4^+CD25^+Foxp3^+$cells, which are called Tregs in a TGF-β1 and retinoic acid-dependent manner and play an important role in immune tolerance.[16,17] This evidence indicates that HSCs activation can trigger Treg cell derivation. Moreover, the Treg cell frequency increases during chronic liver injury, which contributes to the formation of liver fibrosis and cirrhosis through immune tolerance.[18,19] Based on this evidence and our data, we propose that GSG may play an important antifibrotic role by suppressing Treg cell differentiation.

In our study, we found that the numbers of Treg cells in the mouse livers in the GSG-treatment groups were decreased compared with that in the SR group, which indicated that GSG may play an important antifibrotic role, in part by suppressing Treg cell differentiation, which may help to break immune tolerance. Downregulation of Treg cells may clear away fibrous connective tissue. Previous reports have demonstrated that Treg cells function in a cytokine-dependent manner.[20,21] We found that the expression levels of IL-6, TNF-α, and IL-1β in the SR group were lower than those in the high- and medium-dose GSG groups, and TGF-β1 expression showed the opposite results. When Treg cell differentiation was inhibited and immune tolerance was overcome, the levels of IL-6, TNF-α, IL-1β increased, and TGF-β1 levels decreased, which contributed to liver regeneration and rehabilitation. However, the balance of these cytokines may promote the resolution of liver cirrhosis.

Although this study found a connection between HSCs activation and Treg cell derivation, the mechanism underlying the suppressive effect of GSG on Treg derivation was not explored. Overall, our findings provide insight into the antifibrotic mechanism of GSG, the understanding of which is essential for this medicine in clinical settings.

Conflict of Interest

The authors have declared no conflicts of interest.

Author Contributions

Liu YM performed the experiments. Shi HB wrote and modified the manuscript. Liu YR and Shi HL performed the flow cytometry experiments. Ren F, Chen Y, Chen DX and Lou JL provided the chemical profile of GSG analyzed by HPLC. Duan ZP guided the experimental design and manuscript writing.

REFERENCES

1. Talwalkar JA, Kamath PS. Influence of recent advances in medical management on clinical outcome of cirrhosis. Mayo Clin Proc 2005;80:1501-1508.
2. Friedman SL, Bansal MB. Reversal of hepatic fibrosis—fact or fantasy? Hepatology 2006;43(2 Suppl 1):S82-S88.
3. Wang YD, Han T, He JR. Research progress of chronic liver fibrosis treatment with extract from traditional Chinese medicine. Med Recapitul (Chin) 2012;124:4228-4231.
4. Xie JR, Zhu Y, Zhu WR, Wang JB. Research progress of antifibrotic mechanism of traditional Chinese medicine. Inf Tradit Chin Med (Chin) 2011;28:147-149.
5. Zhang QH, Zhang CR. The effect of GSG on fibrotic marker and liver function in patients with chronic hepatitis B. Guangdong Med J (Chin) 2011;32:118-119.
6. Yue LP, Ma H, Jia JD. Effects of Ganshuang Granules on gene and protein expression of collagen Ⅰ, collagen Ⅲ and tissue inhibitor of metalloprotenase1 in HSC-T6 cells. Chin J Integr Tradit West Med Liver Dis (Chin) 2007;17(2):85-87.
7. Dunham RM, Thapa M, Velazquez VM, Elrod EJ, Denning TL, Pulendran B, et al. Hepatic stellate cells preferentially induce $Foxp3^+$ regulatory T cells by production of retinoic acid. J Immunol 2013;190:2009-2016.
8. Tu CT, Wang JY. Recent advances in our understanding of the molecular mechanisms of liver fibrosis. Chin J Hepatol (Chin) 2014;22:5-8.
9. Yang MD, Chiang YM, Higashiyama R, Asahina K, Mann DA, Mann J, et al. Rosmarinic acid and baicalin epigenetically derepress peroxisomal proliferator-activated receptor c in hepatic stellate cells for their antifibrotic effect. Hepatology 2012;55:1271-1281.
10. Asahina K, Tsai SY, Li P, Ishii M, Maxson RE Jr, Sucov HM, et al. Mesenchymal origin of hepatic stellate cells, submesothelial

cells and perivascular mesenchymal cells during mouse liver development. Hepatology 2009;49:998-1011.

11. Li Y, Wang J, Asahina K. Mesothelial cells give rise to hepatic stellate cells and myofibroblasts via mesothelial-mesenchymal transition in liver injury. Proc Natl Acad Sci 2013;110:2324-2329.
12. Tsukamoto H, Zhu NL, Wang J, Asahina K, Machida K. Morphogens and hepatic stellate cell fate regulation in chronic liver disease. J Gastroenterol Hepatol 2012;27(Suppl2):S94-S98.
13. Puche JE, Saiman Y, Friedman SL. Hepatic stellate cells and liver fibrosis. Compr Physiol 2013;3:1473-1492.
14. Friedman, SL. Hepatic stellate cells: protean, multifunctional, and enigmatic cells of the liver. Physiol Rev 2008;88:125-172.
15. Radaeva S, Wang L, Radaev S, Jeong WI, Park O, Gao B. Retinoic acid signaling sensitizes hepatic stellate cells to NK cell killing via upregulation of NK cell activating ligand RAE1. Am J Physiol Gastrointest Liver Physiol 2007;293:G809-G816.
16. Denning TL, Wang YC, Patel SR, Williams IR, Pulendran B. Lamina propria macrophages and dendritic cells differentially induce regulatory and interleukin 17-producing T cell responses. Nat Immunol 2007;8:1086-1094.
17. Coombes JL, Siddiqui KR, Arancibia-Cárcamo CV, Hall J, Sun CM, Belkaid Y, et al. A functionally specialized population of mucosal CD103$^+$ DCs induces Foxp3$^+$ regulatory T cells via a TGF-beta and retinoic acid-dependent mechanism. J Exp Med 2007;204:1757-1764.
18. Huang CH, Jeng WJ, Ho YP, Teng W, Chen WT, Chen YC, et al. Increased regulatory T cells in patients with liver cirrhosis correlated with hyperbilirubinemia and predict bacterial complications. J Gastroenterol Hepatol 2014;30:775-783.
19. Li J, Jia M, Liu Y, She W, Li L, Wang J, et al. Telbivudine therapy may shape CD4$^+$ T-cell response to prevent liver fibrosis in patients with chronic hepatitis B. Liver Int 2015;35:834-845.
20. Manicassamy S, Reizis B, Ravindran R, Nakaya H, Salazar-Gonzalez RM, Wang YC, et al. Activation of beta-catenin in dendritic cells regulates immunity versus tolerance in the intestine. Science 2010;329:849-853.
21. Sun CM, Hall JA, Blank RB, Bouladoux N, Oukka M, Mora JR, et al. Small intestine lamina propria dendritic cells promote *de novo* generation of Foxp3 Treg cells via retinoic acid. J Exp Med 2007;204:1775-1785.

(Accepted April 10, 2015; First Online November 5, 2015)
Edited by YUAN Lin